

## Characteristics of skeletal muscle chloride channel CIC-1 and point mutant R304E expressed in Sf-9 insect cells

D.St.J. Astill<sup>a,b</sup>, G. Rychkov<sup>a,b</sup>, J.D. Clarke<sup>a</sup>, B.P. Hughes<sup>a</sup>, M.L. Roberts<sup>b</sup>,  
A.H. Bretag<sup>a,b,\*</sup>

<sup>a</sup> Centre for Advanced Biomedical Studies, University of South Australia, North Terrace, Adelaide, South Australia 5000, Australia

<sup>b</sup> Department of Physiology, The University of Adelaide, Adelaide, South Australia 5005, Australia

Received 20 October 1995; accepted 22 November 1995

### Abstract

Using the baculovirus system, the skeletal muscle chloride channel, CIC-1 (rat), and a point mutant replacing arginine 304 with glutamic acid were expressed at high levels in cultured Sf-9 insect cells. Whole-cell patch-clamping revealed large inwardly rectifying currents with maxima up to 15 nA inward and 2.5 nA outward. Saturation was evident at voltage steps positive to +40 mV whilst steps negative to -60 mV produced inactivating currents made up of a steady state component and two exponentially decaying components with  $\tau_1 = 6.14 \pm 0.92$  ms,  $\tau_2 = 36.5 \pm 3.29$  ms (S.D.)  $n = 7$  for steps to -120 mV. Currents recorded in the outside-out patch configuration were often unexpectedly large and up to 5% of whole-cell currents obtained in the same cell, suggesting an uneven channel distribution in the plasmalemma of Sf-9 cells. The pharmacology of a number of chloride channel blockers, including anthracene-9-carboxylate (A9C), niflumate, and perrhenate, was investigated and showed for the first time that perrhenate is an effective blocker of CIC-1 and that it has a complex mechanism of action. Further, the potency of A9C was found to be dependent on external chloride concentration. As in studies on muscle cells themselves, blockade was rapidly effective and easily reversible, except when applying the indanyloxyacetate derivative, IAA94/95, which took up to 10 min to act, and, consistent with an intracellular site of action, was difficult to reverse by washing. Mutation of the highly conserved arginine at position 304 to a glutamic acid did not significantly alter the behaviour of the channel.

**Keywords:** Chloride channel; Mutagenesis; Muscle; Blocker; Baculovirus

### 1. Introduction

Chloride channels of the CIC family have now been demonstrated in many cell types where they have been implicated in a variety of functions including volume regulation [1], ion secretion [2], ion balance [3] and stabilisation of membrane potential [4]. Within this family, the CIC-1 type is expressed primarily in skeletal muscle [4] and there is a very high level of homology between different species (rat, mouse and human). Normal function of these channels is essential for the control of excitability in skeletal muscle, mutations in CIC-1 having been linked to the muscle hyperexcitability diseases, Thomsen's autosomal dominant myotonia congenita and Becker's recessive generalised myotonia, [5–8].

Complementary DNAs encoding the rat and human CIC-1 protein have previously been successfully expressed in *Xenopus* oocytes [4], HEK293 [9] and COS cells [4]. Currents through the expressed CIC-1 channels have been observed in the former two cell types and are characterised by inactivation at hyperpolarising potentials and saturation at depolarising potentials, in accordance with macroscopic currents seen in muscle cells. Expression of cDNA incorporating the point mutations found in human pedigrees leads to abnormal currents further supporting the contention that CIC-1 is the channel defective in the above-mentioned diseases [4]. Interestingly, the kinetics of the currents recorded differ for channels expressed in oocytes and HEK cells [4,9].

In the present work, wild-type rat CIC-1 and a point mutant (glutamic acid replacing arginine at position 304) were expressed at high levels in cultured insect cells using a baculovirus vector (cf. [10] and [4]). Whole-cell patch-

\* Corresponding author. Fax: +61 8 3022389; e-mail: a.bretag@unisa.edu.au.

clamping was used directly on Sf-9 cells expressing the ClC-1 proteins, revealing macroscopic currents typical of those found in other heterologous expression systems and quite comparable with those recorded from muscle cells. Similar results are presented for the first time using the outside-out patch configuration. Patch longevity and stability has been a feature of our study allowing excellent freedom from current drift and ready ability to return to control conditions following tests. Characteristics of chloride currents in Sf-9 cells were compared with those observed in other rectifying channels and susceptibility to various chloride channel blocking compounds was assessed. We show that these blockers have characteristic and differential actions on instantaneous and steady state currents. Evidence is also presented for heterogeneous distribution of ClC-1 in the Sf-9 plasmalemma.

## 2. Materials and methods

### 2.1. Protein expression

The original *clc-1* cDNA in vector pBluescript (Stratagene) [4] was provided by Professor Thomas Jentsch and Dr. Kalus Steinmeyer of the Centre for Molecular Neurobiology, Hamburg, Germany and was designated, in our laboratory, TJJClone. Insert cDNA was excised with *Xba*I and *Cl*aI, end-filled using Klenow DNA polymerase and blunt end ligated into *Bam*HI cleaved, end filled baculovirus transfer vector pBacPAK1 (Clontech). Clones were isolated containing insert DNA in forward and reverse orientations which were designated pDA1BVR and pDA2BVR, respectively. Insert DNA in pDA1BVR was subjected to PCR using primers (CLCXBA, CLCTTH) designed to amplify the region of the open reading frame from the start codon (nt 84) to 30 bp downstream of the unique *Tth*111I site (nt 387). Upstream primer CLCXBA was designed to remove the upstream untranslated region whilst incorporating an *Xba*I site immediately prior to the ATG. PCR products were separated from unincorporated primers, nucleotides and target DNA by electrophoresis on a 1% TAE agarose gel. The product band was then excised and extracted using Qiaex resin (QIAGEN), cleaved with *Xba*I and *Tth*111I and ligated into similarly cleaved and purified TJJClone. Modified *clc-1* in its entirety was then excised from pBluescript using *Xba*I and *Kpn*I, gel purified and ligated into similarly cleaved pBacPAK8 (Clontech). This third construct was designated pDA6bvr. Orientation of the insert DNA and integrity of all constructs was established by restriction analysis and DNA sequencing (double stranded dye-labelled terminator method, Applied Biosystems, primers Bac1 (PBPRIM1) and Bac2 (PBPRIM2) for pDA1BVR and pDA2BVR, PBPRIM1 and TTHSEQ for pDA6BVR).

Recombinant baculoviruses were produced in IPLB-Sf-

21 insect cells grown in Grace's insect cell culture medium (Gibco) supplemented with lactalbumin hydrolysate, yeast-olate (Difco) and 10% bovine fetal serum (CSL). Monolayer cultures of insect cells were incubated at 28–30°C in air and passaged at ca. 80% confluence (twice weekly). Cells to be infected were seeded at low density (40–50% confluence) and incubated overnight before inoculation. Each vector was introduced into the Sf-21 cells along with linearised baculovirus (Bac6, Clontech, cf. [11]) using lipofectin (Gibco BRL) mediated transformation as recommended by the supplier. After 2 days incubation, the culture supernatants were collected and used to produce isolated plaques in Sf-21 monolayers following the method described by King and Possee [12]. Four clones derived from each of the three constructs were used to infect fresh Sf-21 monolayers. Following incubation (5–7 days) the cells were collected, washed in PBS (Dulbecco A, Oxoid) and virus DNA extracted as described by King and Possee [12]. PCR using the Bac1 and 2 sequencing primers was used to confirm transfer of the relevant insert DNA into the viral genome in all clones and restriction analysis of PCR products using *Eco*RV and *Tth*111I confirmed the predicted orientation of the *clc-1* reading frame with respect to the polyhedrin promoter. Four clones of each recombinant virus were amplified by infection of Sf-21 monolayers in 25 cm flasks. Resulting virus stocks were titred by standard plaque assay [12] and were then screened for protein production in Sf-9 insect cells (chosen for their amenability to electrophysiological study [10]) cultured as for the Sf-21 cells and treated as follows. Sf-9 cells in 35 mm dishes were infected with each clone at a multiplicity of infection (moi) of 60–100 and incubated for 48 h. Cells were then harvested, washed and resuspended in PBS to a concentration of  $10^4$  cells/ $\mu$ l. Following sonication in a bath type sonicator, an equal volume of 2  $\times$  PAGE sample buffer (100 mM Tris-Cl, 200 mM dithiothreitol, 4% SDS, 0.2% bromophenol blue, 20% glycerol (pH 6.8)) was added. Samples (15  $\mu$ l) were electrophoresed on discontinuous polyacrylamide gels [13] (4% stacking gel, 9% resolving gel). Proteins were visualised by staining for 30 min in coomassie blue followed by overnight destaining. After analysis of protein expression, one clone of each recombinant virus was selected for use in further experiments, designated BVDA1 (complete cDNA forward orientation), BVDA2 (complete cDNA reverse orientation) and BVDA6 (5' UTR deleted). Putative glycosylation of the expressed protein was assessed using the glycosylation inhibitor, tunicamycin (Boehringer Mannheim) as described by King and Possee [12].

Large scale working stocks of virus clones BVDA2 and BVDA6 were produced by infection of 50 ml suspension cultures of Sf-21 cells with each virus at 0.2 moi. Cultures were harvested after 6–7 days incubation and the cells removed by centrifugation (3000  $\times$  g/10 min). Virus-containing supernatants were stored at 4°C. Titres of working stocks were determined using standard plaque assay.

## 2.2. Site-directed mutagenesis

5' modified cDNA was excised from pDA6BVR and subcloned into vector pALTER-1 (Promega) using *Bam*HI and *Kpn*I. Mutagenesis of the arginine residue at position 304 to glutamic acid was performed using the Altered Sites System (Promega) following the manufacturers protocols and using mutagenic primer JCR304E. The primer serves to change the arginine codon TCG to TTC and eliminates an *Mn*II restriction site. Verification of mutants was by PCR of the sequence spanning codons 272 to 393 using primers JCSEQ1 and JCSEQ2 followed by direct sequencing, using the same primers (Applied Biosystems, dyelabelled terminator protocol) and restriction analysis using *Mn*II. Mutated cDNA was then excised from pALTER-1 using *Xba*I and *Kpn*I and subcloned into pBacPAK8 to produce pDA6-R304E. Virus production and verification was as described above finally resulting in baculovirus expression vector BVDA6-R304E.

## 2.3. Oligonucleotide primer sequences

CLCTTH 5'-TCCTT CTCAG CACAC GTCCC AGCG AT-3'; CLCXBA 5'-ATTCT AGATG GAGCG GTCCC AGTCC CAG-3'; JCR304 5'-GGAAT TACTG GGAGG GATTG TTTGC-3'; JCSEQ1 5'-GCCGT GGGGG GTCGG TTGCT GT-3'; JCSEQ2 5'-ATAGA GCAGG CGGTG CTTAG C-3'; PBPRIM1 5'-ACCAT CTCGC AAATA AATAA G-3'; PBPRIM2 5'-ACAAC GCACA GAATC TAGCG-3'; TTHSEQ 5'-GCTAA CATAG TCCAT GCACC A-3'.

## 2.4. Electrophysiology

Sf-9 insect cells were seeded at low density in 35 mm petri dishes and incubated, as described for Sf-21 cells, until ca. 50% confluence (24–48 h). Cells were then infected with virus clones BVDA2, BVDA6 or BVDA6-R304E at a moi of 50 and incubated for 24–30 h. Following incubation, infected cells were seeded onto glass coverslips and, until used for patch-clamping, were maintained at room temperature in cell culture medium for up to 10 h. Immediately prior to patch-clamping, cells were rinsed in bath solution to remove excess culture medium. The bath solution contained (mM) NaCl (160), MgCl<sub>2</sub> (2), CaCl<sub>2</sub> (2), glucose (10) and Hepes-Na (10) at pH 7.4. For low chloride bath solution (4 mM) NaCl was replaced by Na-glutamate and MgCl<sub>2</sub> was replaced by MgSO<sub>4</sub>. Whole-cell and outside-out patch-clamping was performed directly on cells 28–34 h post infection using a List EPC7 patch clamp amplifier and associated standard patch-clamping equipment. Electrodes of 2–4 MΩ were pulled from borosilicate glass on a Kopf two step puller and were filled with a solution containing (mM) KCl (40), K-glutamate (120), EGTA-Na (10) and Hepes-Na (10) at pH 7.2. Data were collected using an IBM compatible PC and

pCLAMP v5.5 software (Axon Instruments) which also enabled such analysis as extraction of exponential and steady state components from original current records. Potentials listed are pipette potentials corresponding to the convention, intracellular potential relative to outside zero. Junction potentials estimated to be –14 mV between standard pipette and bath solutions were not corrected for, unless otherwise stated, in the presentation of our results. Experiments were performed at room temperatures of 21 ± 1°C. In conductance blocking experiments, anthracene-9-carboxylate (A9C, Aldrich), perrhenate (Koch-Light), 2,4-dichlorophenoxyacetate (2,4-D, Sigma), an indanyloxyacetate derivative (IAA94/95 from D.W. Landry, see [14]) and niflumate (Squibb) were prepared as the sodium salts from their corresponding acids, by neutralisation with an equivalent amount of NaOH (1 M), allowing ready aqueous dissolution. Dose–response curves were fitted using the sigmoidal dose–response (variable slope) function of GraphPad Prism (GraphPad Software Inc., San Diego, CA). In some experiments, NaCl in the bath solution was replaced by glucose on an equi-osmolar basis and, in others, all cations except for H<sup>+</sup> in either or both the bath and pipette were replaced by Tris. When iodide was used as the blocker, NaI replaced NaCl on an equimolar basis in the bath solution. Under the conditions employed in the present study, background conductance of the Sf-9 cell membrane was relatively low (cf. [15]). Where necessary, pentobarbitone (Faulding, 0.5 mM) was used to block native anion channels [15], which allowed them to be readily discriminated from expressed channels.

## 3. Results

### 3.1. Protein expression

PAGE analysis of Sf-9 cells revealed a clearly visible protein band with an apparent *M<sub>r</sub>* of ca. 116 kDa (Fig. 1) which was present only in cells infected with virus clones expected to express CIC-1 (BVDA1, BVDA6, BVDA6-R304E). Cells infected with virus clones not anticipated to express CIC-1 (BVDA2) did not produce the 116 kDa protein but otherwise showed a protein profile similar to that seen in other infected cells and different from uninfected cells. Similarly, the 116 kDa protein was not detectable in cells infected with wild type *AcMNPV* control virus (results not shown). Although all BVDA1 and BVDA6 (wt and mutant) clones expressed the 116 kDa protein, the level of expression varied. One clone of each type was selected at random from those clones giving the best expression. A consistently and markedly higher yield of CIC-1 was obtained in cells infected with BVDA6 (wt and mutant, 5' UTR deleted) compared to BVDA1 (Fig. 1). Investigation of post translational processing using the glycosylation inhibitor tunicamycin failed to reduce the apparent *M<sub>r</sub>* of the protein. Harvesting of cells at various

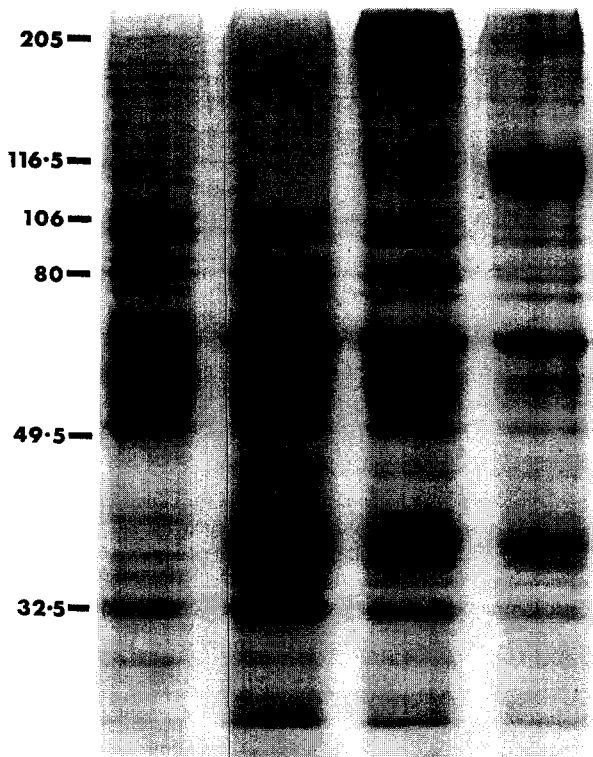


Fig. 1. A Coomassie blue stained 9% SDS-PAGE of whole cell protein extracts from Sf-9 cells at 40 h post infection. Extracts made from a standardised number of cells were applied to each lane. Lane 1: uninfected cells. Lane 2: infected with negative control virus (BVDA2.1). Lane 3: infected with virus containing complete *cdc-1* cDNA (BVDA1.7). Lane 4: infected with virus containing *cdc-1* cDNA with 5' untranslated sequence deleted (BVDA6.3). Molecular weight markers (kDa) are indicated. Lanes 3 and 4 show expression of a protein at an apparent  $M_r$  of 116 kDa.

time points, from 18–170 h pi, showed that CIC-1 was detectable by coomassie staining from approximately 30 h pi, with maximum expression at around 40 h. After ca. 72 h incubation, protein yield decreased rapidly concomitant with virus-induced host cell lysis.

### 3.2. Electrophysiology

Gigaohm seals were easily obtained on Sf-9 cells, whether infected or uninfected, in standard bath solution. In the cell-attached patch, resistance was always high ( $> 10 \text{ G}\Omega$ ) and no voltage-dependent single channel activity was observed. Nor was there any obvious conductance nonlinearity that might have indicated voltage-dependent activity of channels with a conductance too small to be resolved at the single channel level.

Whole-cell mode was achieved from cell-attached patches by the application of negative pressure to the pipette and could regularly be maintained for an hour or more. Evaluation of control cells (uninfected and BVDA2 infected) then revealed small whole-cell leakage currents, constant with time and almost linear with respect to voltage (Fig. 2), that could be evoked by the voltage step

protocol illustrated. Maximum currents were typically in the range of 150 pA inward and outward. Under certain conditions, such as hypotonicity, larger currents were able to be induced which could be attributed to the activity of native volume regulatory anion channels. This activity was readily blocked by pentobarbitone, leaving the above-mentioned low amplitude leakage currents. In contrast, cells infected with BVDA6 (wt and mutant) and expressing CIC-1, produced large inwardly rectifying currents with maxima up to 15 nA inward and 2.5 nA outward (Fig. 2) that were unaffected by pentobarbitone ( $> 10 \text{ mM}$ ). These inwardly rectifying currents had a reversal potential of  $-23.9 \pm 1.4 \text{ mV}$  (S.D.,  $n = 25$ ) which, when corrected for a junction potential of  $-14 \text{ mV}$ , was close to that calculated from the Nernst equation ( $-36.6 \text{ mV}$ ) for the imposed chloride gradient. Deactivation of peak inward current to a steady state was evident for potential steps negative to  $-60 \text{ mV}$  whilst saturation of outward currents

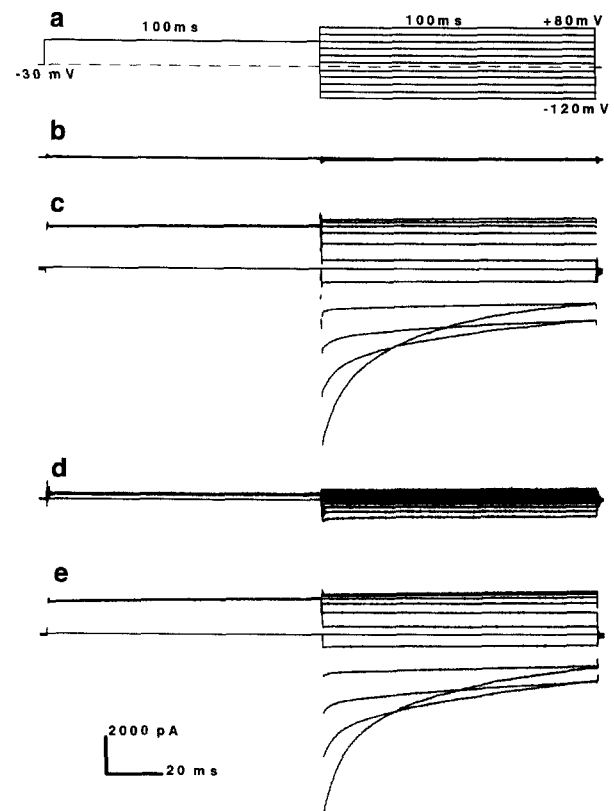


Fig. 2. Whole-cell patch-clamp currents due to expressed CIC-1 in a cultured Sf-9 insect cell. (a) Voltage step protocol: a holding potential of  $-30 \text{ mV}$  was maintained for at least 2 s between pulses comprising an activating prepulse to  $+40 \text{ mV}$  for 100 ms followed in each cycle by 100 ms test pulses ranging from  $-120$  to  $+80 \text{ mV}$  in  $20 \text{ mV}$  increments. (b) Currents elicited by the voltage step protocol (illustrated in a) in an Sf-9 cell not expressing CIC-1, having been infected with negative control virus (BVDA2.1). (c) Currents (as in b) but elicited in an Sf-9 cell expressing CIC-1, having been infected with virus containing *cdc-1* cDNA with 5' untranslated sequence deleted (BVDA6.3). (d) Currents from the same cell (as in c) after addition of perrhenate ( $10 \text{ mM}$ ) to the bath solution. (e) Restoration of currents, again in the same cell (as in c), 5 min after washout with normal bath solution.

was observed for steps more positive than +40 mV. Maximal inward current was obtained by activation of channels using a 100 ms prepulse to +40 mV prior to each step in the voltage protocol. Neither deactivation nor saturation of outward currents were significantly modified by bathing solutions or pipette solutions in which all small cations other than  $H^+$  were substituted by Tris. Higher  $Ca^{2+}$  or  $Mg^{2+}$  concentrations of up to 20 mM in the bathing solution or up to 2 mM in the pipette were, likewise, without significant effect.

Fig. 3 shows the  $I$ - $V$  relationship for both the instantaneous and steady state currents illustrated in Fig. 2. The deactivating inward currents (Fig. 2) evoked by strongly hyperpolarising voltage steps are made up of three readily resolvable components, two decreasing exponentially, plus a steady state component. Kinetic behaviour of deactivating currents in the R304E mutant was not noticeably different from wild-type where pulses to  $-120$  mV elicited exponentially decaying components with time constants  $\tau_1 = 6.14 \pm 0.92$  and  $\tau_2 = 36.5 \pm 3.29$  ms (S.D.,  $n = 7$ ). For lesser hyperpolarisations the fast component becomes even faster and the slow becomes slower, e.g., at  $-60$  mV,  $\tau_1 = 2.8 \pm 0.53$  and  $\tau_2 = 94.6 \pm 23.7$  ms (S.D.,  $n = 7$ ) until, eventually, they become unresolvable as they merge with the capacitive transient and the steady state current, respectively, for still less negative pulses. Some drift in the characteristics of these currents was noted in the first 20 min after perforation of the patch to enter the whole-cell recording mode. Peak and steady state currents steadily increased and kinetics slowed slightly, mainly as a result of an increased prominence of the second component. By 20 to 30 min post perforation, excellent stability was achieved with little or no further drift in any observed current parameter. When very long lasting (seconds) hyperpolarising pulses were used, a third exponential with a

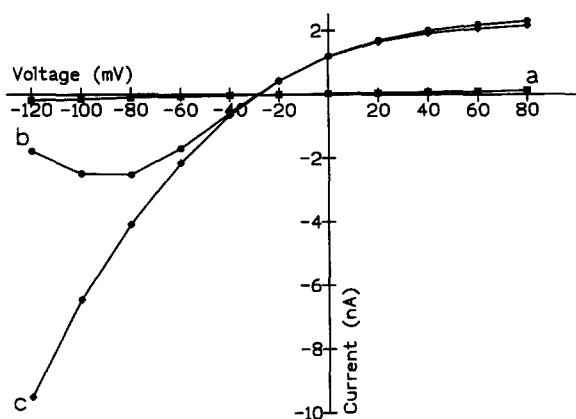


Fig. 3. Current-voltage curves from control Sf-9 cells and cells expressing ClC-1. Sets of whole-cell currents, as illustrated in Fig. 2c, were used to produce current-voltage curves from (a) a typical Sf-9 cell infected with negative control virus (BVDA2.1) compared with steady state (b) and peak (c) currents obtained from a different cell infected with virus containing *clc-1* cDNA with 5' untranslated sequence deleted (BVDA6.3).

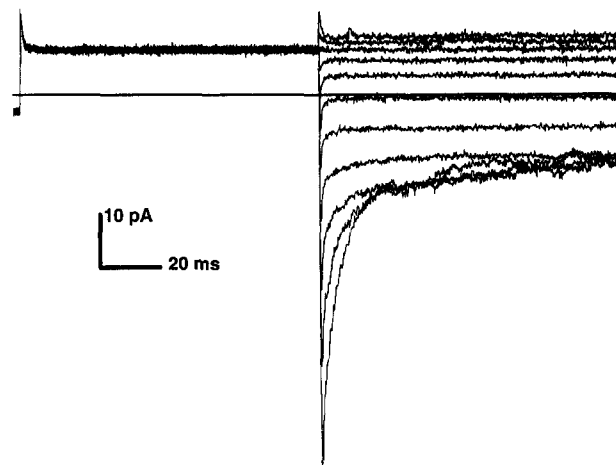


Fig. 4. Outside-out patch-clamp currents due to expressed ClC-1 in a cultured Sf-9 insect cell. Currents were elicited by the step protocol illustrated in Fig. 2a. The peak inward current of approx. 70 pA for the  $-120$  mV step was obtained from an Sf-9 cell which had a maximum whole-cell inward current of approx. 1.5 nA for the same hyperpolarising step.

time constant of the order of several hundred milliseconds could be extracted from the deactivating currents.

Outside-out patches could, in many cases, be obtained by pulling the pipette away from a cell in which whole-cell recording had been established. From control cells, outside-out patches occasionally showed single channel activity that was not voltage-dependent and which could be blocked by pentobarbitone. Large voltage-dependent currents were only ever seen in outside-out patches from appropriately infected cells which had previously displayed similar macroscopic currents in the whole-cell patch. Peak amplitudes of the deactivating currents varied considerably from patch to patch but in 10% of positive patches ( $n > 40$ ) were as much as 5% of the original whole-cell current amplitude (Fig. 4) despite microscopic observation showing no evidence of tethers, no visible vesicle at the pipette tip and predicted surface area having diminished to much less than 1% of that of the whole-cell [16]. Kinetics were as described for whole-cell currents. Interestingly, there was sometimes an increase of up to two times in current amplitude during the first few minutes following formation of the outside-out patch after which all current parameters were stable. No discrete current steps indicative of single channel events, other than those that could be attributed to the native anion channels, were ever seen in these patches.

Known blockers of chloride conductance in whole muscle preparations, such as perrhenate (Fig. 2), A9C (Fig. 5), 2,4-D and iodide (results not shown) reduced inward and outward currents in both whole-cell and outside-out patch configurations toward levels seen in control cells. When perrhenate was applied, block of instantaneous currents was simply proportionally related to concentration (Fig.

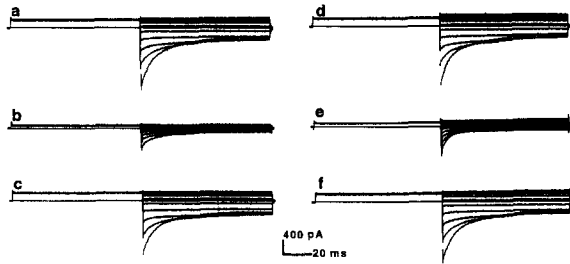


Fig. 5. Whole-cell patch-clamp currents, elicited by the same voltage protocol as in Fig. 2a, showing the effects of chloride channel blockers. (a) Currents elicited in an Sf-9 cell expressing ClC-1. (b) Currents from the same cell 5 min after addition of A9C (0.1 mM) to the bath. (c) Restoration of currents, again in the same cell, 10 min after washout with normal bath solution. (d,e,f) A similar sequence of patch-clamp currents illustrating blocking action by niflumate (1 mM) and subsequent washout.

6a), but steady state currents appear to be increased by concentrations of about 1 mM and decreased by higher concentrations (see also Fig. 6c). By contrast, A9C always appears to block both instantaneous and steady state currents to similarly increasing extents with increasing concentration (Fig. 6b). Dose–response curves for the blocking action of perrhenate and A9C are illustrated in Fig. 6c, where the calculated  $IC_{50}$  for instantaneous currents is 1.1 mM and 7  $\mu$ M, respectively. The potency of A9C was found to be markedly increased when using low external chloride concentrations. When applied in bath solution containing 4 mM  $Cl^-$  the same changes in current amplitudes occurred at lower concentrations and the calculated  $IC_{50}$  was reduced to 1.6  $\mu$ M (Fig. 6c). Preliminary results with niflumate, a potent blocker of red cell anion exchange, indicate that it reduces currents in a similar fashion to A9C (Fig. 5) with an  $IC_{50}$  of 50  $\mu$ M. All of these blockers were rapidly effective (within seconds, as bath solution was exchanged) and were totally reversible on washout. When high concentrations (mM) of another chloride conductance blocker, IAA94/95, were applied, at least 10 min elapsed before block became apparent, and reversal was difficult to obtain, even with extensive washing. Potency and characteristics of block by these various agents was not different in the R304E mutant.

#### 4. Discussion

The ClC-1 protein is expressed at high levels in the baculovirus-Sf-9 insect cell system. Expression of this channel using cRNA injection in *Xenopus* oocytes has previously been found to require the replacement of the 5' untranslated region of the message with the equivalent region of the ClC-0 channel from *Torpedo californica* [4]. In Sf-9 cells, the channel is expressed without modification of the message although the level of expression is significantly enhanced by the complete removal of the upstream untranslated sequence. Previous studies of expression of foreign genes using the baculovirus polyhedrin promoter

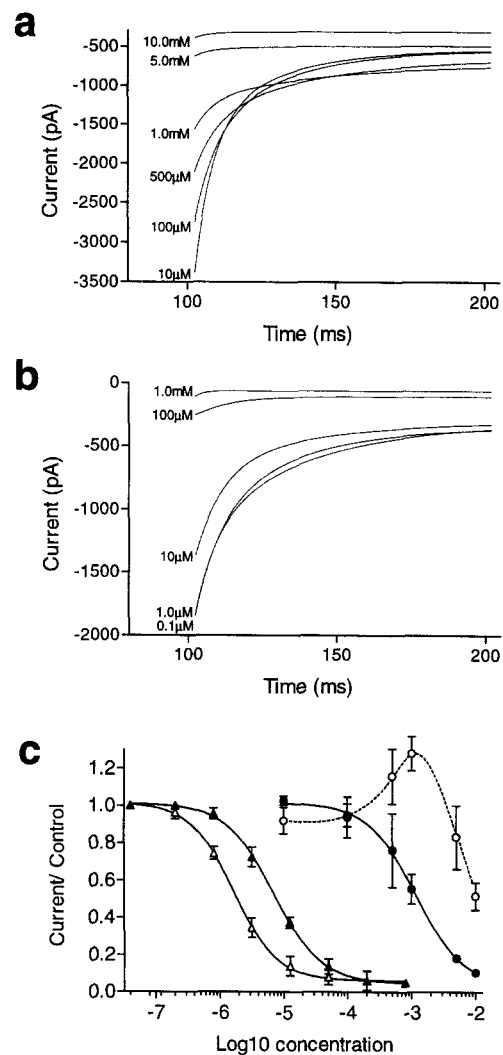


Fig. 6. Dose–response relationships for the blocking action of perrhenate and A9C. (a) Effect of blocking doses of perrhenate ranging from 10  $\mu$ M to 10 mM on whole-cell currents elicited by a 100 ms voltage test pulse to  $-120$  mV immediately following a 100 ms prepulse to  $+40$  mV (part of the voltage step protocol shown in Fig. 2a). Each current is shown as the sum of its steady-state and fast and slow exponential components and represents the line of best fit to the original current record. All currents were recorded from the one whole cell patch on a single cell, allowing sufficient time for equilibration of the response at each new concentration. (b) Whole-cell currents, represented as in (a), in the presence of blocking doses of A9C ranging from 0.1  $\mu$ M to 1 mM. Again allowing time for equilibration, all currents were recorded from the one whole-cell patch on a single cell. (c) Dose–response curves for the blocking action of A9C (168 mM chloride, filled triangles; 4 mM chloride, open triangles) and perrhenate (filled circles) on normalised peak instantaneous currents. Current amplitudes were determined from summation of extracted components, as in (a), extrapolated back to the beginning of the test pulse. Solid lines represent sigmoidal dose–response functions fitted as described in Section 2. The dose–response curve for the blocking effect of perrhenate on extracted steady state currents is illustrated for comparison (open circles). In this case the broken line represents a fit to the data by an arbitrary cubic spline. In each case points represent means  $\pm$  S.E. for data obtained from three different cells, except for perrhenate at 0.5 mM where results from only two cells have been utilised.

have indicated that the viral sequence between the initiation site and the natural polyhedrin ATG (50 base pairs) must be preserved for optimal expression [17]. Inclusion of the 5' untranslated region (83 base pairs) of *clc-1* does not interfere with this viral sequence. However, the spacing between the transcription initiation site and the ATG is reduced from 127 bp in BVDA1 to 32 bp in BVDA6 constructs. While no definitive studies have been performed to investigate the effect of spacing between these elements, it is possible that keeping the separation close to that found naturally in the viral genome may be a factor in optimising the transcription and/or translation of foreign sequences. Alternatively, and given the experience with expression in *Xenopus* oocytes [4], we favour the view that the 5' untranslated region of *clc-1* contains some *cis*-acting elements which directly inhibit its transcription and/or translation in insect and amphibian cells.

Although its DNA sequence predicts an unprocessed mass of 110 kDa, on PAGE the CIC-1 protein from Sf-9 cells has an apparent  $M_r$  of ca. 116 kDa. This might reflect its hydrophobic nature, extremely hydrophobic proteins commonly running at anomalous molecular weights. Alternatively, the expressed CIC-1 could have been subjected to some post-translational processing event(s). For example, Kieferle et al. [2] have convincingly demonstrated glycosylation of CIC proteins in a mammalian-derived cell free system. Cultured insect cells are known to be capable of performing all post-translational modifications performed by mammalian cells, including palmitylation, acylation and glycosylation, albeit not always authentically (for review see [12]). Electrophoresis and Western blotting of native CIC-1, extracted directly from rat muscle, has recently been reported [18]. The native protein also migrates with an apparent  $M_r$  higher than predicted, however the authors were unable to determine definitively whether or not the protein was glycosylated *in vivo*. Our investigation with tunicamycin suggests that CIC-1 is not glycosylated in Sf-9 cells. Furthermore, when compared with CIC-1 expressed in HEK293 cells, its electrophysiological behaviour suggests that, if any processing differences exist between these cell lines, then they are inconsequential.

In agreement with the high level of CIC-1 expression indicated by PAGE analysis, patch clamping demonstrates the appearance of large, voltage-dependent currents consistent with the presence of numerous, selective chloride channels. These currents are independent of large changes in divalent cation concentration and of the absence of  $\text{Na}^+$  and  $\text{K}^+$ . Voltage dependence and deactivation and activation kinetics of the currents are in good agreement with the macroscopic chloride currents found in whole muscle [19] as well as being very similar to those found in transfected HEK293 cells [9]. Just as for the HEK293 cells, kinetics of the currents in Sf-9 cells are faster than those found when CIC-1 is expressed in *Xenopus* oocytes. We have, as yet, no mechanistic explanation for the various components of

deactivation of the inward currents nor for the property of inward rectification. Analogies with the inward rectifier potassium channel can, however, be drawn, where similar current–voltage relations have been obtained as a result of potential-dependent channel block by intracellular  $\text{Mg}^{2+}$  and extracellular  $\text{Cs}^+$  [20]. It is also worth noting that a volume regulatory  $\text{Cl}^-$  channel from cultured human small intestine epithelial cells (Intestine 407) displays an apparent deactivation and block due to intracellular  $\text{Mg}^{2+}$  [21]. Lack of a significant effect when  $\text{Ca}^{2+}$  and  $\text{Mg}^{2+}$  concentrations were manipulated or when all small cations other than  $\text{H}^+$  were substituted by Tris, suggests that this particular mechanism is not responsible for similar characteristics in CIC-1.

Stability of the patch-clamp seal in both whole-cell and outside-out configurations combined with the longevity of recordings makes the Sf-9 preparation ideal for pharmacological studies and determination of metabolic control of CIC-1. For example, entire dose–response curves and washout with return to control conditions are currently being performed on the one preparation. Both instantaneous and steady state inward and outward currents are blocked by various compounds, e.g., A9C, perrhenate, 2,4-D and iodide, which are known to block chloride conductance in whole muscle. Considering the possibility that channel environment and, perhaps, modulatory protein subunits could alter the pharmacological behaviour of CIC-1, the  $\text{IC}_{50}$  determined for A9C in the present study compares well with that determined in rat muscle *in situ* [22] and suggests that any such influences are insubstantial. Niflumate has not previously been described as a blocker of muscle chloride channels although it and the related diphenylaminecarboxylates are well known as chloride transport inhibitors in other tissues [23–26]. It is possible that the mechanism of block for some of these agents is simple occlusion of the channel pore, but for others, such as perrhenate where channel kinetics appear to be affected, channel gating must be modified.

The increase in potency of A9C in low chloride solution could simply reflect competition between this blocker and  $\text{Cl}^-$  for a common binding site, implying that A9C exerts its action within the channel pore, however alternative explanations are also possible. One such explanation would be that binding of A9C to a site remote from the pore could induce a reversible change in protein conformation which destroys one or more chloride binding site. Conversely, when chloride is bound to its site(s) the channel may be unable to undergo this A9C induced conformational change and/or bound blocker may be displaced. Under this scenario an equilibrium between chloride and A9C binding would exist which would clearly be shifted in favour of the blocker with significantly reduced  $\text{Cl}^-$  concentration. An intramembrane site of action for A9C has previously been suggested [22].

These blockers are active as rapidly as solution change can be effected (within seconds). By contrast, IAA94/95

added to the bath solution is slow to act and is then poorly reversible. A similar time course has been obtained when using IAA94/95 on the isolated rat diaphragm to induce chloride channel block myotonia (Bretag, A.H., unpublished observations). These results are consistent with an intracellular site of chloride channel block by IAA94/95, for which additional evidence has been presented by Weber-Schürholz et al. [27], although other interpretations are also possible. Altogether our results underline the appropriateness of the Sf-9 system expressing CIC-1 as a model for the study of the skeletal muscle cell membrane chloride conductance and add additional weight to the already strong case that CIC-1 comprises the major chloride permeation pathway in these membranes.

Arginine 304 is highly conserved throughout the CIC family. The currently predicted topology of the channel places this residue within the cytoplasm at the base of the fifth membrane spanning domain, previously designated D6 [4]. Reversing the charge of this residue did not detectably alter the behaviour of the channel with respect to its kinetics, selectivity or sensitivity to the blockers tested. These results suggest that this residue, despite being highly conserved, does not participate in the gating process and is unlikely to be exposed in the pore of CIC-1. It apparently also does not form part of the ligand binding site(s) for any of the blocking agents used in this study.

In cell-attached and outside-out patches, the absence of obvious single channel events attributable to CIC-1 conforms with previous studies where a single channel conductance of the order of 1 pS has been suggested on the basis of noise analysis [9]. We are, however, surprised by the lack of non-linear currents in any of our cell-attached patches (many hundreds) and by the relatively enormous currents seen in some of our outside-out patches (up to 5% of whole cell currents). One explanation for these results could be that an interaction with the glass somehow inactivates CIC-1 channels inside a pipette tip in a cell-attached patch. Another could be heterogeneity in distribution of CIC-1 in the plasmalemma of the Sf-9 cells, with CIC-1 occurring in extended homogeneous arrays. Gigaohm seals might only be possible if the pipette contacts the lipid bilayer and not if it contacts such a protein raft, so that channels could never be captured inside a successful cell-attached patch. Conversely, outside-out patches could contain anything from no CIC-1 channels up to an extensive raft of them, thus accounting for the variation in the observed ensemble current. The dominant negative effect of CIC-1 mutations in Thomsen's autosomal dominant myotonia congenita has been ascribed to a multimeric (trimeric or tetrameric) association of CIC-1 monomers [28]. Alternatively, a protein raft or array could display an equivalent dominant negative effect due to nearest neighbour interactions between normal and mutant proteins. Depending on the type of interaction between monomers, on the number of monomers that must cooperate to form a single channel and on the type of packing in an array,

variable proportions of the potential maximum channel number could be eliminated by incorporation of defective monomers (cf. [29,30]).

## Acknowledgements

We are extremely grateful to Prof. T.J. Jentsch and Dr. K. Steinmeyer of the Centre for Molecular Neurobiology, Hamburg, for providing the rat CIC-1 clone, to Dr. D.W. Landry of the College of Physicians and Surgeons, Columbia University, New York, for providing the IAA94/95 and to Squibb Pharmaceuticals for providing the niflumic acid. D.St.J.A. holds a 'Ross Stuart Postgraduate Scholarship' of the Muscular Dystrophy Association of South Australia. Supported by the Neuromuscular Research Foundation of the Muscular Dystrophy Association of South Australia, the Australian Research Council and the Research Committee of the University of South Australia.

## References

- [1] Thiemann, A., Gründer, S., Pusch, M. and Jentsch, T.J. (1992) *Nature* 356, 57–60.
- [2] Kieferle, S., Fong, P., Bens, M., Vandewalle, A. and Jentsch, T.J. (1994) *Proc. Natl. Acad. Sci. USA* 91, 6943–6947.
- [3] Uchida, S., Sasaki, S., Furukawa, T., Hiraoka, M., Imai, T., Hirata, Y. and Marumo, F. (1993) *J. Biol. Chem.* 268, 3821–3824.
- [4] Steinmeyer, K., Ortland, C. and Jentsch, T.J. (1991) *Nature* 354, 301–304.
- [5] Koch, M.C., Steinmeyer, K., Lorenz, C., Ricker, K., Wolf, F., Otto, M., Zoll, B., Lehmann-Horn, F., Grzeschik, K.-H. and Jentsch, T.J. (1992) *Science* 257, 797–800.
- [6] George, A.L.J., Crackower, M.A., Abdalla, J.A., Hudson, A.J. and Ebers, G.C. (1993) *Nature Genet.* 3, 305–310.
- [7] Heine, R., George, A.L.J., Pika, U., Deymeier, F., Rüdel, R. and Lehmann-Horn, F. (1994) *Human Mol. Genet.* 3, 1123–1128.
- [8] Lorenz, C., Meyer-Kleinfeld, C., Steinmeyer, K., Koch, M.C. and Jentsch, T.J. (1994) *Human Mol. Genet.* 3, 941–946.
- [9] Pusch, M., Steinmeyer, K. and Jentsch, T.J. (1994) *Biophys. J.* 66, 149–152.
- [10] Bear, C.E., Li, C., Kartner, N., Bridges, R.J., Jensen, T.J., Ramajee Singh, M. and Riordan, J.R. (1992) *Cell* 68, 809–818.
- [11] Kitts, P.A., Ayres, M.D. and Possee, R.D. (1990) *Nucleic Acids Res.* 18, 5667–5672.
- [12] King, L.A. and Possee, R.D. (1992) *The Baculovirus Expression System: A Laboratory Guide*, Chapman and Hall, London.
- [13] Laemmli, U.K. (1970) *Nature* 227, 680–685.
- [14] Landry, D.W., Reitman, M., Cragoe, E.J.J. and Al-Awqati, Q. (1987) *J. Gen. Physiol.* 90, 779–798.
- [15] Birnir, B., Tierney, M.L., Howitt, S.M., Cox, G.B. and Gage, P.W. (1992) *Proc. R. Soc. Lond. B Biol. Sci.* 250, 307–312.
- [16] Sakmann, B. and Neher, E. (1983) in *Single-Channel Recording* (Sakmann, B. and Neher, E., eds.), pp. 37–52, Plenum Press, New York.
- [17] Matsuura, Y., Possee, R.D., Overton, H.A. and Bishop, D.H.L. (1987) *J. Gen. Virol.* 68, 1233–1250.
- [18] Gurnett, C.A., Kahl, S.D., Anderson, R.D. and Campbell, K.P. (1995) *J. Biol. Chem.* 270, 9035–9038.
- [19] Fahlke, C. and Rüdel, R. (1995) *J. Physiol. (Lond.)* 482, 355–368.



- [20] Hille, B. (1992) *Ionic Channels of Excitable Membranes*, 2nd Edn., Sinauer, Sunderland.
- [21] Oiki, S., Kubo, M. and Okada, Y. (1994) in  $\text{Cl}^-$  Channel: Molecular and Cellular Physiology (Okada, Y., Oiki, S., Yamagishi, S. and Hama, K., eds.), pp. 56–58, National Institute for Physiological Sciences, Okazaki.
- [22] Palade, P.T. and Barchi, R.L. (1977) *J. Gen. Physiol.* 69, 879–896.
- [23] Cousin, J.L. and Motaïs, R. (1979) *J. Membr. Biol.* 46, 125–153.
- [24] Wängemann, P., Wittner, M., Di Stefano, A., Englert, H.C., Lang, H.J., Schlatter, E. and Greger, R. (1986) *Pflügers Arch.* 407 (Suppl. 2), S128–S141.
- [25] Bretag, A.H. (1987) *Physiol. Rev.* 67, 618–724.
- [26] Greger, R. (1990) *Methods Enzymol.* 191, 793–809.
- [27] Weber-Schürholz, S., Wischmeyer, E., Laurien, M., Jockusch, H., Schürholz, T., Landry, D.W. and Al-Awqati, Q. (1993) *J. Biol. Chem.* 268, 547–551.
- [28] Steinmeyer, K., Lorenz, C., Pusch, M., Koch, M.C. and Jentsch, T.J. (1994) *EMBO J.* 13, 737–743.
- [29] Bretag, A.H., Davis, B.R. and Kerr, D.I.B. (1974) *J. Membr. Biol.* 16, 363–380.
- [30] Bretag, A.H. and Kerr, D.I.B. (1975) *Z. Naturforsch. C.* 30, 535–537.